



Vascular alteration in relation to fosfomycine: In silico and in vivo investigations using a chick embryo model



Hadi Tavakkoli^{a,*}, Reza Attaran^a, Ahmad Khosravi^b, Zohreh Salari^c, Ehsan Salarkia^b, Shahriar Dabiri^d, Seyedeh Saedeh Mosallanejad^e

^a Department of Clinical Science, School of Veterinary Medicine, Shahid Bahonar University of Kerman, Kerman, Iran

^b Leishmaniasis Research Center, Kerman University of Medical Science, Kerman, Iran

^c Obstetrics and Gynecology Center, Afzalipour School of Medicine, Kerman University of Medical Sciences, Kerman, Iran

^d Afzalipour School of Medicine & Pathology and Stem Cells Research Center, Kerman University of Medical Sciences, Kerman, Iran

^e Afzalipour School of Medicine & Biochemistry Department, Kerman University of Medical Sciences, Kerman, Iran

ARTICLE INFO

Keywords:

Anti-angiogenic
Chorioallantoic membran
DNA promoter
Fosfomycin
In silico
VEGF-A

ABSTRACT

Fosfomycin residues are found in the egg following administration in the layer hen. In this regard, some aspects of embryo-toxicity of fosfomycin have been documented previously. The exact mechanism by which fosfomycin causes embryo-toxicity is not clearly understood. We hypothesize that fosfomycin may alter vasculature as well as normal expression of genes, which are associated with vascular development. Therefore, the present study aimed to address these issues through in silico and in vivo investigations. At first, embryo-toxicity and anti-angiogenic effects of fosfomycin were tested using computerized programs. After that, fertile chicken eggs were treated with fosfomycin and chorioallantoic membrane vasculature was assessed through morphometric, molecular and histopathological assays. The results showed that fosfomycin not only interacted with VEGF-A protein and promoter, but also altered embryonic vasculature and decreased expression level of VEGF-A. Reticulin staining of treated group was also confirmed decreased vasculature. The minor groove of DNA was the preferential binding site for fosfomycin with its selective binding to GC-rich sequences. We suggested that the affinity of fosfomycin for VEGF-A protein and promoter as well as alteration of the angiogenic signaling pathway may cause vascular damage during embryonic growth. Hence, veterinarians should be aware of such effects and limit the use of this drug during the developmental stages of the embryo, particularly in breeder farms. Considering the anti-angiogenic activity and sequence selectivity of fosfomycin, a major advantage that seems to be very promising is the fact that it is possible to achieve a sequence-selective binding drug for cancer.

1. Introduction

The normal growth of the avian embryo inside the egg is linked with the normal development of the vascular plexus. Administration of some drugs in breeder poultry flocks may alter embryonic growth and cause teratogenic effects [1]. It is imperative to consider that the genesis and expansion of the vascular plexus are associated with various mechanisms and pathways. Regular expression of angiogenic-regulating gene such as Vascular Endothelial Growth Factor A (VEGF-A) is one of the most important mechanism involved in the development of vascular plexus. VEGF-A is produced by mesenchymal tissues and binds to tyrosine kinase receptors such as VEGF-R1, -R2 and -R3 [2–4].

Bacterial pathogens can cause a variety of diseases in chicken farms, particularly in breeders, and are responsible for significant worldwide economic losses. Methods for management and controlling bacterial diseases in poultry include good biosecurity practices, immunization strategies and certain medicinal treatments. Although a great deal of research effort has been focused on developing non-medicinal strategies for bacterial diseases, antibiotics have remained the major means of control in many countries [5].

Fosfomycin (FO) is a bactericidal antibiotic, which is widely used in poultry production in various regions across the globe such as South and Central America and Asia. Fosfomycin has the smallest molecular mass of all antibiotics. It is a phosphonic acid derivative which

Abbreviations: CAM, chorioallantoic membrane; CFA, capillary fractional area; FO, fosfomycin; GAPDH, glyceraldehyde-3-phosphate dehydrogenase; H&E, hematoxylin and eosin; HH, Hamburger and Hamilton; qPCR, quantitative real-time PCR

* Corresponding author at: Department of Clinical Science, School of Veterinary Medicine, Shahid Bahonar University of Kerman, 22 Bahman Boulevard, Pajouhesh Square, Kerman, 7616914111, Iran.

E-mail address: tavakkoli@uk.ac.ir (H. Tavakkoli).

<https://doi.org/10.1016/j.biopha.2019.109240>

Received 13 May 2019; Received in revised form 10 July 2019; Accepted 16 July 2019

0753-3322/ © 2019 The Authors. Published by Elsevier Masson SAS. This is an open access article under the CC BY-NC-ND license (<http://creativecommons.org/licenses/by-nc-nd/4.0/>).

possesses broad spectrum activity against gram-negative and gram-positive bacteria.

Since the embryo-toxicity of drugs is of great concern, some aspects of FO toxicity have been previously assessed in several researches [6–11]. It is well established that following administration in laying hens, FO residues are found in the eggs [12]. Various factors have been associated with the toxicity of FO, but the exact mechanism by which FO possesses embryo-toxicity is not yet clearly understood.

One of the most important mechanisms influencing the normal growth of the embryo is angiogenesis [13–15]. Hence, we hypothesized that FO may alter the angiogenesis and factors which are associated with vascular development. Until now, this possible anti-angiogenic effect has not been evaluated in the literature. This investigation was designed to address the following issues:

- A Does FO cause vascular alteration?
- B Does FO interact with proteins and gene promoters which have important roles in angiogenesis?
- C What is the binding mode between FO and angiogenic proteins and promoters?
- D Does FO alter expression of genes associated with angiogenesis?

To answer these questions, a chick embryo model was applied and *in silico* analysis was performed to evaluate the anti-angiogenic activity of FO. The results were also accompanied with *in vivo* study to assess the effect of drug on vasculature and molecular expression.

Since our preliminary investigation (*in silico* and molecular assays) showed relationships between FO and VEGF-A, the interaction between FO and VEGF-A was evaluated in the present study.

2. Materials and methods

This section is described in terms of A) *in silico* investigation and B) *in vivo* investigation.

2.1. *In silico* investigation

Computerized evaluation of FO toxicity as well as its interaction with protein and gene promoter, which are associated with angiogenesis, was performed. After molecular modeling, ligand and receptor docking was performed to reveal the anti-angiogenic potential of FO.

2.1.1. Embryo-toxicity evaluation of FO

The molecular structure of FO was obtained in molecular data file format (MDL Molfile) from the pubchem database (<https://pubchem.ncbi.nlm.nih.gov/>, PubChem CID: 93095). The FO structure was uploaded onto PASS online software to evaluate the embryo-toxicity of the drug based on structural model (<http://www.pharmaexpert.ru/passonline/>). The toxicity and corresponding Pa (probability to be active) and Pi (probability to be inactive) values were recorded.

2.1.2. Molecular modeling

Possible interaction of FO with VEGF-A protein and promoter were identified. The functional domain sequence of VEGF-A protein (*Gallus gallus*, Gene ID: 395909) was acquired from the National Center for Biotechnology Information (NCBI) GenBank and a suitable template structure was identified by blasting across the NCBI database. Crystal structure of human VEGF-A receptor binding domain (target template) was obtained from the RCSB Protein Data Bank (PDB code: 4KZN). The crystal structure of VEGF-A (4KZN) contains the native ligands. Protein model of VEGF-A (*Gallus gallus*) was generated using the SWISS-MODEL (<https://swissmodel.expasy.org/>) according to the user template model. The accuracy, reliability and stability of the SWISS-MODEL server have been previously validated by the EVA method [16].

Moreover, we assessed whether FO might also interact with WTL binding sites (a promoter site located on VEGF-A gene) [17]. For this

purpose, the promoter sequences of VEGF-A gene was downloaded in FASA format from the NCBI database (Gene ID: 395909). The data was transferred to PROMO server for the identification of putative transcription factor binding sites in DNA sequences [18,19]. The binding site of WTL was simulated using the 3D-DART (<http://haddock.chem.uu.nl/dna/dna.php>). This server provides a convenient means of generating custom 3D structural model of DNA with control over the various parameters [20]. The simulated WTL binding sites of *Gallus gallus* was named canonical B-DNA.

Receptors and ligand were prepared for docking by adding partial charges and hydrogen. In order to identify the potential binding of FO to VEGF-A protein and WTL binding site, a docking study was performed using AutoDockVina [21]. All docked poses of FO were ranked based on the binding docking energies and the lowest energy conformation was selected for the subsequent study. Receptors and ligand binding were visualized and schematic diagrams of interactions were obtained. Amino acids and nucleotides showing interactions with FO were identified.

We also decided to perform cross-dockings to identify the preferential binding mode for FO in a way that the targets possess a known groove or intercalation gap. To this end, the Protein Data Bank was searched for DNA-ligand complexes and two molecular structures were chosen: 1DNE (structure of a dodecamer DNA d(CGCGATATCGCG)2 in complex with netropsin) and 1Z3F (structure of a hexamer DNA d(CGATCG)2 in complex with ellipticine). Netropsin is an antibiotic that typically binds with DNA through minor groove interaction [22], while ellipticine is an intercalating agent with antitumor property [23,24]. The structures of the 1DNE and 1Z3F are shown in Fig. 1. The DNA binding modes between FO-canonical B-DNA, netropsin-1DNE and ellipticine-1Z3F were compared to each other.

In the next step, a cross-docking with FO, 1DNE receptor and 1Z3F receptor was performed. Following the separation of the coordinates of the ligands (netropsin and ellipticine) from the coordinates of the receptors (1DNE and 1Z3F), polar hydrogens were added using AutoDock Tools. In order to include the entire DNA fragment, a 3D grid box of size 30 × 28 × 32 with a resolution of 1 Å was made. After the grid box was centered on the macromolecule, docking was performed.

Finally, a validation stage was performed by self-dockings between 1DNE, 1Z3F and their original ligands. This stage was considered as the main indication of docking accuracy.

2.2. *In vivo* investigation

In this category, anti-angiogenic property of FO was evaluated in the chick embryo using CAM and molecular assays.

2.2.1. Materials

Fertile chicken eggs (Ross 308, with the average egg-weight of 56.3 ± 0.7 g) were supplied by Mahan Breeder Farm, Kerman, Iran. The breeder flock was kept under optimal rearing condition. FO was purchased from RooyanDarou Pharmaceutical Company (Tehran, Iran) and was dissolved in sterile phosphate buffered saline. A stock solution was prepared and stored in small aliquots for future use. Phosphate-buffered saline (PBS) and paraffin were obtained from Merck, Darmstadt, Germany. RNA extraction kit (High Pure RNA Tissue Kit) and SYBR Green kit (FastStart SYBR Green Master) were purchased from Roche Diagnostics GmbH, Mannheim, Germany. cDNA synthesis kit (AccuPowerCycleScript RT PreMix dN6) was obtained from BIONEER, Seoul, South Korea.

2.2.2. CAM assay

The present study was performed according to the suggested European Ethical Guidelines for the care of animals in experimental investigations in line with the guidelines of the Veterinary School of Shahid Bahonar University and was approved (project no. 95-P/11/20) by the Clinical Sciences' Committee of the Research Council of Shahid

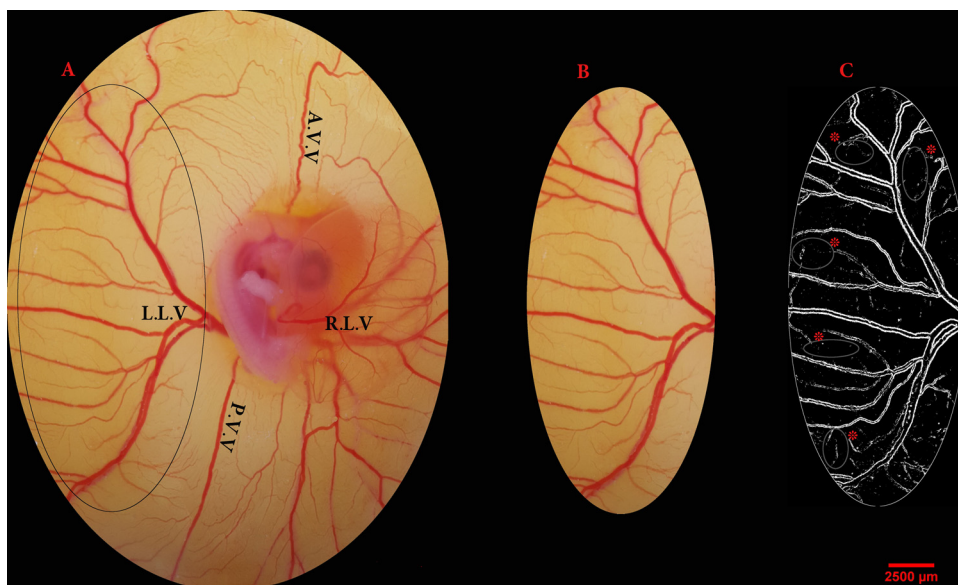


Fig. 1. Calculation of the mean capillary area (MCA) by estimating changes in the chorioallantoic capillary plexus. (A) Certain area within the left-lateral vitelline plexus is selected. (B) Selection has been converted to a binarized format. (C) Five fields (asterisk) without any branch vessels were identified and the percentages of the areas containing white pixels were calculated. The white pixels represent the areas containing blood in the original pictures. A.V.V., anterior vitelline vein; P.V.V., posterior vitelline vein; R.L.V., right-lateral vitelline plexus; L.L.V., left-lateral vitelline plexus.

Bahonar University, Iran.

CAM assay was performed to evaluate the *in vivo* anti-angiogenic potential of FO. In brief, fertilized chicken eggs (Ross 308) were incubated at 37 °C in 60–80% humidity for 24 h. Egg shells were cleaned with 70% ethanol and then a pinpoint hole was made through the blunt pole of the shell. Fifty microliter of either FO or sterile phosphate buffered saline, as sham control, was dropped in the shell membrane using a Hamilton syringe. FO was applied at a dose of 160 mg/kg egg-weight (the recommended dose in poultry). The fertilized eggs were re-injected at two different time points: 24 and 48 h following the first injection. The egg shell was sealed with melted paraffin and the eggs were re-subjected to incubation under the mentioned conditions.

On Hamburger–Hamilton developmental stage 22–24 (day 4 of the incubation period), the egg shell and shell membrane were aseptically removed to expose the surface of the CAM by peeling a 25 × 25 mm window on the egg. A minimum of ten eggs per group were used. High quality images (4000 × 3000 pixels) were captured using a stereomicroscope (Luxeo 4D Stereozoom Microscope, Labomed, CA, USA) and analyzed in a 14.5-inch PC (Intel Core i3-390 M, 2.66 GHz). Then, the CAM was cut with scissors (2.5 cm in diameter) and surrounding embryonic tissues were surgically removed. The cut CAM was used as a sample for molecular assay.

2.2.3. Analysis of the CAM response

Software packages including ImageJ® 1.48 (National Institutes of Health, Bethesda, Maryland, USA), Digimizer® 4.3.0 (MedCalc Software, Mariakerke, Belgium) and MATLAB® (Mathworks/Matlab R2015a) were used to analyze the vascular structure of the CAM.

At first, a uniform area (2800 × 3000 pixels) was extracted from the captured images and then an area of interest (310 mm² containing 1320 × 3084 pixels) was identified in the left-lateral vitelline plexus. The area of interest was determined using ImageJ software. Efforts were made to select the constant areas in order to avoid subjectivity in image analysis. Therefore, the area of interest was located in the left-lateral vitelline plexus. This method has been applied in various investigations [25,26]. The parameters including vessels area and total vessels length were calculated in the selected vascular bed.

Anti-angiogenic activity of FO was also quantified by estimating changes in the CAM capillary plexus. For this purpose, pictures were prepared according to the following procedure. A certain area (310 mm² within the left-lateral vitelline plexus), after contrast enhancement, was selected and converted to a binarized image. Five fields having no branch vessels were selected and the percentages of the areas

containing white pixels were calculated. These areas are named capillary fractional areas (CFA) and represent the areas containing blood in the original pictures. Finally, the mean capillary area (MCA) was calculated from the mean of all CFA areas.

2.2.4. Molecular assay

Quantitative real-time PCR (qPCR) assay was performed to evaluate the effect of FO on the expression of VEGF-A gene. Glyceraldehyde-3-phosphate dehydrogenase (GAPDH) was used as a reference gene in each reaction [27,28]. The sequences of the forward and reverse primers are listed in Table 1. Total RNA was extracted from the CAM of chick embryos using High Pure RNA Tissue Kit and was subsequently reverse-transcribed into complementary DNA (cDNA) with AccuPowerCycleScript RT PreMix dN6 kit according to the manufacturer's protocol. The qPCR was performed on the Rotorgene Cyclor system (Rotorgene 3000 cyclor system, Corbett Research, Sydney, Australia) with hot-start treatment step at 95 °C for 1 min and then fluorescence intensity was recorded during 40 cycles (10 s at 95 °C, 15 s at 60 °C and 20 s at 72 °C). Expression levels were calculated using the comparative Ct ($2^{-\Delta\Delta C_t}$) method.

2.2.5. Histopathological evaluation

Chicks' CAM samples were fixed in 10% buffered formalin and then samples were washed through graded concentrations of ethanol and put in paraffin block and the samples were dehydrated, cleared and embedded in paraffin wax. In next step sections were cut with a rotary microtome at 5 mm thicknesses, then stained with hematoxylin and eosin (H&E) and reticulin (Merck_Germany, code number: 1.01510.0050).

Table 1

The sequences of the forward and reverse primers for quantitative real-time PCR.

Gene (<i>Gallus gallus</i>)	Sequence (5'–3')	Product size (bp)
VEGF-A		86
Forward	caattgagaccctgggtggac	
Reverse	tctcatcagaggcacacagg	
GAPDH		176
Forward	cctctctggcgaagtccaag	
Reverse	ggtcacgctcctggaagata	

2.3. Statistical analysis

Statistical analysis was performed using SPSS software, version 20 (SPSS Inc., Chicago, IL, USA). Independent sample *t*-test was applied to evaluate the significance of differences in vascular parameters, MCA and gene expression. A *p*-value of less than 0.05 was considered statistically significant.

3. Results

3.1. Embryo-toxicity of fosfomycin in PASS

The structure of FO was subjected to embryo-toxicity evaluation through the PASS online server. The acquired results were filtered with Pa (probability to be active) and Pi (probability to be inactive) values. High Pa and Pi values were observed for embryo-toxicity of FO (Pa = 0.847, Pi = 0.009).

3.2. Conformational analysis of simulated receptors

The 3D structures of VEGF-A protein (*Gallus gallus*) and canonical B-DNA (WTI binding site, *Gallus gallus*) were simulated by the SWISS-MODEL and 3D-DART, respectively (Fig. 2B and D). The quality of protein structure was checked by analyzing residue-by-residue geometry and overall structure geometry using PROCHECK (<http://servicesn.mbi.ucla.edu/Verify3D/>). The Ramachandran plot is presented in Fig. 2C. PROCHECK source information revealed that 90.4% of the residues were in most favored regions, 8.2% of the residues were in additional allowed regions, 1.4% of the residues were seen in generously allowed regions, and 0.0% of residues were in disallowed regions. These data confirm that a good quality model would be expected. The structural parameters of VEGF-A model were as follows: number of amino acids = 83, molecular weight = 9537.99, total number of negatively charged residues (Asp + Glu) = 12 and total number of positively charged residues (Arg + Lys) = 7.

As previously mentioned, the WTI binding site sequences were selected and simulated for docking assay in order to find out any base sequences specific for binding to FO. According to PROMO output and blasting results, the binding site was located on chromosome 3 (NC_006090.5) of the *Gallus gallus* (GRCg6a, GCF_000002315.5) at location 30797911 to 30797919. The canonical B-DNA sequences consisted of 9 base pairs. Specific bases from the 5'-end in DNA duplex included 5'-d (GGGAGGGGG)2. The other properties of simulated B-DNA were as follows: Molecular Weight = 2884.9, GC content = 89% and melting temperature = 34 °C.

3.3. Affinity of fosfomycin for VEGF-A and promoter

Molecular docking assay was conducted to clarify the binding pattern between FO and its targets. Docking results showed that the active site of VEGF-A protein was interacted with the FO molecule (affinity = -6.8 kcal/mol) (Fig. 3A). As presented in the binding model, FO was bound to the active site of VEGF-A by van der Waals interaction and five hydrogen bonds between cysteine 3, cysteine 79 and threonine

5 (Fig. 3B and C).

Docking result confirmed that FO could also bind to the canonical B-DNA, which was located on VEGF-A gene (affinity = -7.9 kcal/mol) (Fig. 3D). The van der Waals interaction and hydrogen bonds between FO and nucleotide (guanine and cytosine) are presented in Fig. 3E and F.

3.4. Binding mode of fosfomycin

As explained in the method section, cross-dockings were carried out with 1DNE and 1Z3F receptors, instead of original ligands, to identify the preferential binding modes for FO. The results are illustrated in Fig. 4.

The results showed that among two distinct binding modes of interaction (intercalation between base pairs or groove recognition), FO bound to the minor groove in all tested DNA. It is important to note, however, the crystallographic structure of 1Z3F shown in Fig. 4B indicates that intercalation interaction is the most accessed binding mode for ellipticine, it can also be observed that crossdocking results shown in Fig. 4E point to a minor groove binding mode for FO.

A summary of the results for FO dockings with the three different DNA receptors is reported in Table 2.

- Canonical B-DNA: simulated WTI binding sites (a promoter site located on VEGF-A gene).
- 1DNE: Structure of the netropsin in complex with DNA.
- 1Z3F: Structure of ellipticine in complex with a 6-bp DNA.
- In modified 1DNE and 1Z3F, their original ligands (netropsin and ellipticine) were removed.
- B-DNA: simulated WTI binding sites (a promoter site located on VEGF-A gene).
- 1DNE: Structure of the netropsin in complex with DNA.
- 1Z3F: Structure of ellipticine in complex with a 6-bp DNA.
- 4KZN: Structure of human VEGF-A receptor binding domain.

Concerning the binding pattern of FO, it is worthwhile to stress that the drug seems to interact selectively with GC-rich sequences. Patterns of hydrogen bonding between FO, canonical BDNA, modified 1DNE and modified 1Z3F are displayed in Fig. 4C–E. In modified 1DNE and 1Z3F, their original ligands (netropsin and ellipticine) were removed. Careful attention to those patterns confirms the assumption that FO interacts only with G and C nucleotides.

3.5. Self-dockings

We also applied a self-dockings assay to prove the accuracy of the results (validation stage). Among the various conformations, nine best-docked conformations were analyzed. Self-dockings results for *N*-acetyl-D-glucosamine, netropsin and ellipticine are presented in Table 2, and the best conformational structure for each docking is demonstrated in Fig. 5. As expected, the applied docking assay was confirmed to be very accurate to predict binding modes for *N*-acetyl-D-glucosamine, netropsin and ellipticine in self-dockings. As revealed in Table 2, 88.0% of runs with *N*-acetyl-D-glucosamine resulted in correct pocket

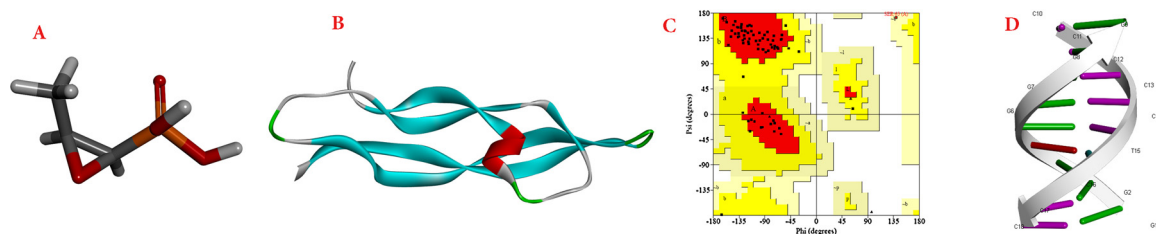


Fig. 2. (A) 3D diagram of fosfomycin. (B) Protein model of VEGF-A (*Gallus gallus*) that was simulated by SWISS-MODEL. (C) Ramachandran plot for protein model of VEGF-A (*Gallus gallus*). Residues in most favored regions are 90.4%. (D) Canonical B-DNA (the binding site of WTI) that was simulated by 3D-DART.

Table 2
Cross-dockings and self-dockings results.

Docking	Receptor	Ligand	Best affinity (kcal/mol)	Correct binding mode ^a	Number of correct prediction ^b
Cross-docking	B-DNA	Fosfomycin	-7.9	Gr	9/9
Cross-docking	1DNE	Fosfomycin	-7.4	Gr	8/9
Cross-docking	1Z3F	Fosfomycin	-6.5	Gr	7/9
Self-docking	4KZN	<i>N</i> -acetyl-D-glucosamine	-7.4	Pocket	8/9
Self-docking	1DNE	Netropsin	-10.0	Gr	9/9
Self-docking	1Z3F	Ellipticine	-7.9	Int	9/9

Gr: Groove recognition; Int: Intercalation.

^a Binding modes of interaction between ligand and receptor.

^b Number of correct binding mode after docking/Number of binding mode.

recognition, with a best binding affinity of -7.4 kcal/mol (Fig. 5A), while all runs with netropsin and ellipticine resulted in minor groove recognition and intercalation interaction, with best binding affinities of -10.0 and -7.9 kcal/mol, respectively (Fig. 5B and C).

- 4KZN: Structure of *N*-acetyl-D-glucosamine in complex with human VEGF-A receptor binding domain.
- 1DNE: Structure of the netropsin in complex with DNA.
- 1Z3F: Structure of ellipticine in complex with a 6-bp DNA.

3.6. Anti-angiogenic property of fosfomycin

We hypothesize that if FO possesses anti-angiogenic property, then it alters normal development of the vasculature. Therefore, the CAM capillary plexus of the treated embryos were analyzed. At the time of evaluation, the treated embryos were at Hamburger–Hamilton developmental stage 22–24. In the control embryos, a normal vasculature was seen around the embryo (Fig. 6A and B). In FO treated embryos, changes were seen in the vascular pattern (Fig. 6C and D).

Data acquired from the analysis of the CAM capillary plexus are demonstrated in Fig. 7. Vessels area and total vessels length were presented in percentage and millimeter, respectively. Reduction in vascular parameters was recognized in FO-treated embryos. Vessels area and total vessels length were significantly lower in FO-treated embryos compared to the control ($p = 0.002$ and $p = 0.012$, respectively).

3.7. Mean capillary area (MCA) following fosfomycin treatment

Fosfomycin was administered onto the chick CAM at 24, 48 and 72 h of incubation period. Anti-angiogenic activity of FO was quantified by estimating MCA. There was a significant reduction in MCA in embryos receiving FO at the dose of 160 mg/kg egg-weight (control embryos, 9.03 ± 1.17 ; FO treated embryos, 5.70 ± 1.06 ; $p = 0.029$).

3.8. Expression of VEGF-A gene following fosfomycin treatment

To verify the anti-angiogenic effect of FO, the expression level of VEGF-A was assessed by qPCR on day 4 of the incubation period. As shown in Fig. 8, angiogenic gene expression was significantly down-regulated in treated embryos.

3.9. Histopathological evaluation

As mentioned earlier, H&E and reticulin staining was performed to evaluate the vascular alterations following FO treatment. As demonstrated in Fig. 9, FO was significantly reduced the vascular plexus in treated CAM compare to control.

4. Discussion

As pointed out in some literature reviews, the incidence of bacterial infections in various breeder poultry farms are rising, which consequently leads to increasing use of antibacterial drugs. The impact of FO in poultry farm with the history of infections has been evaluated in several documented researches [29].

Drug toxicity is of grave concern during embryonic growth. In the present study, embryo-toxicity of FO was evaluated using PASS online server. Regarding the acquired data, high probability of toxicity was predicted. The exact pathway for embryo-toxicity following FO administration is not clearly understood; however, the anti-angiogenic activity of the drug may account for its embryotoxic effect. Since normal intra-uterine development of the embryo is associated with normal development of the vascular plexus, angiogenesis plays a vital role during embryonic growth. In this study, some details about the anti-angiogenic property of FO were assessed and unveiled using in silico technique and in vivo chick embryo model. Herein, we discuss various highlights of the discoveries on the interaction of FO with proteins, DNA and genes, which are associated with angiogenesis.

Nowadays, molecular docking is becoming an important approach to elucidate the interaction between ligands and their targets. Therefore, we use this method for in silico evaluation of FO. It is well known that the VEGF gene and protein are important targets for anti-angiogenic compounds. In this regard, the first to highlight in our study is binding of FO to VEGF-A protein and WTL binding site of *Gallus gallus*. The expression level of VEGF is correlated with different transcription factors. Since the VEGF promoter has several potential WTL binding sites, herein we chose these binding sites to assess whether WTL binding sites might also be affected by FO [17].

The second aspect of the FO interaction is its preferential binding mode to VEGF promoter. In general, binding of small ligands to DNA occurs in two different modes: intercalation binding (binding between

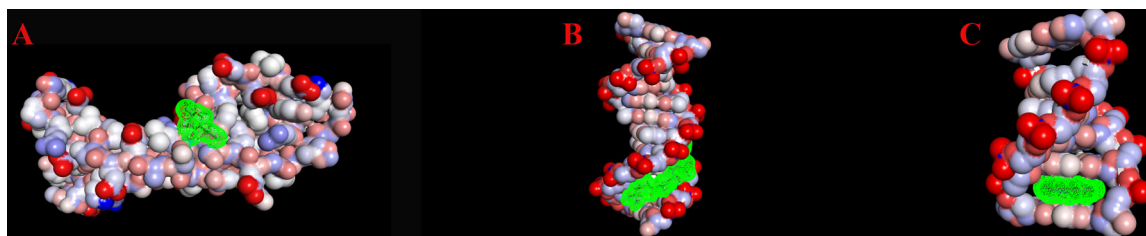


Fig. 5. Validation stage by self-dockings between crystallographic structure of (A) *N*-acetyl-D-glucosamine and 4KZN; (B) Netropsin and 1DNE; (C) Ellipticine and 1Z3F. Binding modes predicted by the docking are in agreement with the binding modes revealed by experiment.

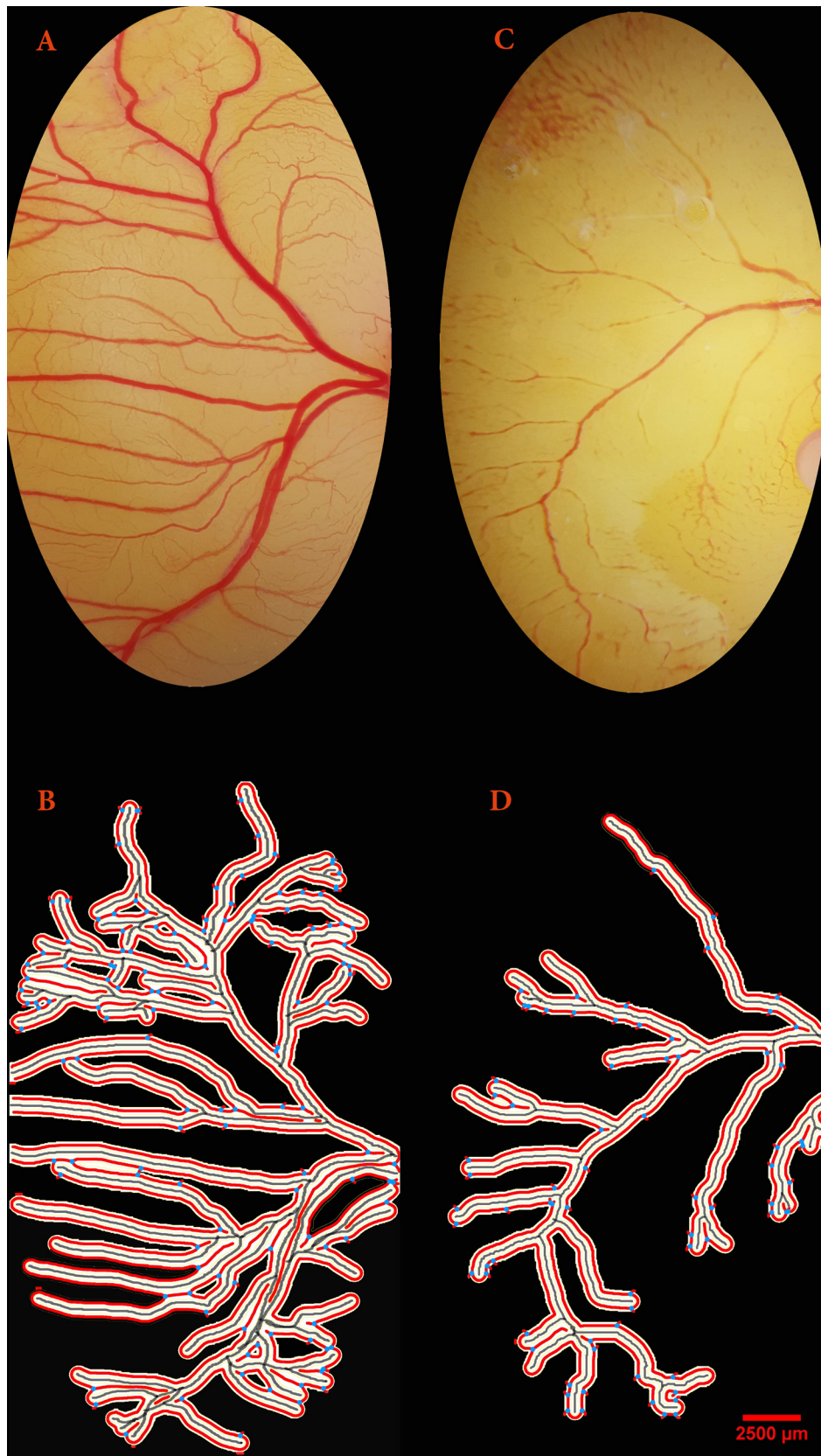


Fig. 6. Chorioallantoic membrane response to fosfomycin. The area of interest (310 mm^2) was extracted from the CAM of the 4-day chick embryo. The images were acquired from the embryos of the control group (A and B) and fosfomycin-treated group at a dose of $160 \text{ mg kg egg-weight}$ (C and D). In fosfomycin-treated embryos, a reduced vasculature was seen.

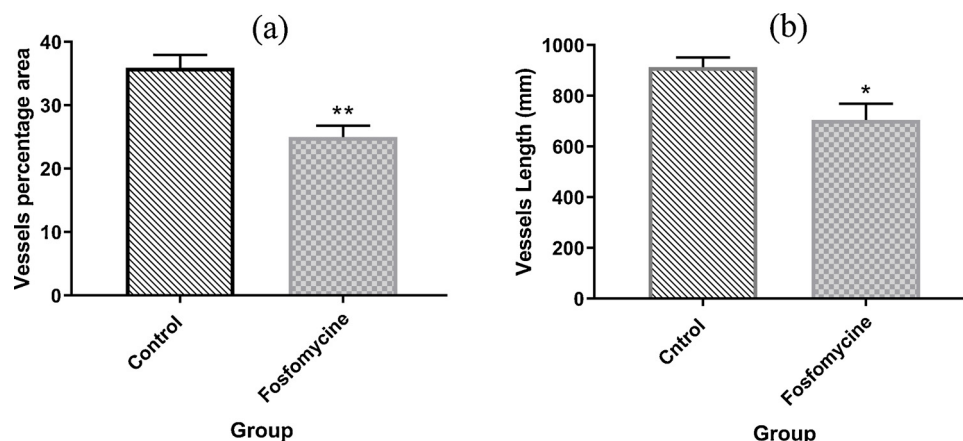


Fig. 7. Analysis of the chorioallantoic capillary plexus. Vessels area (a) and total vessels length (b) are significantly lower in fosfomycin treated embryos compared to control. Fosfomycin was administered at dosage 160 mg/kg egg-weight (error bars show standard error of mean; * $p = 0.002$, ** $p = 0.012$, Independent sample t -test).

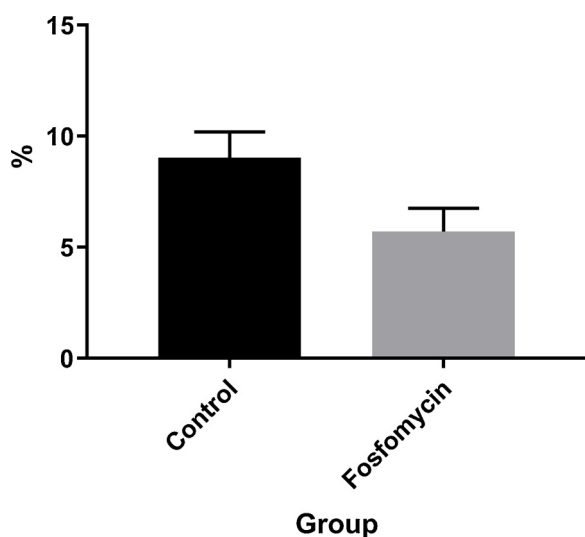


Fig. 8. qPCR results of VEGF-A gene expression following fosfomycin treatment. The expression level of VEGF-A in the chick's chorioallantoic membrane is decreased in the fosfomycin-treated group. The fosfomycin was administered at dosage 160 mg/kg egg-weight (error bars show standard error of mean; * $p < 0.05$, Independent sample t -test).

base pairs) or groove recognition. Although the major groove of DNA provides a much larger binding site with more H-bonding donor and acceptor, most of the small ligands bind to the minor groove [30,31]. Consistently, it was evidently demonstrated in our study that FO bonds to the minor groove of DNA by groove recognition mode.

As previously discussed, since no apparent or little DNA structural alteration was observed following binding, the minor groove recognition by ligand is more similar to a lock-and-key mechanism [30]. On the other hand, it is assumed that lock-and-key interaction depends on a combination of various factors, in which van der Waals contacts assisted by hydrogen bonding play the major role [32]. In our investigation, these intermolecular contacts between FO and canonical B-DNA were obviously observed and so the validity of that assumption was supported.

The third aspect to be discussed is the sequence-selective property of the FO interaction. FO showed a considerable selectivity for binding to GC-rich sequences in the minor groove of the DNA. This issue was confirmed by cross-docking between FO, 1DNE and 1Z3F. 1DNE (DNA complex with netropsin) is a crystallographic structure of DNA with AT-rich sequences, while 1Z3F (DNA complex with ellipticine) is a DNA with GC-rich sequences. In all docked conformations, FO bound to the G

and C nucleotides. Netropsin is known to interact strongly with AT-rich sequences [33]. In the present study, after separating the coordinates of netropsin from 1DNE, the FO still tended to bind with the GC-nucleotides of the 1DNE. This indicates the possibility of achieving sequence-selective binding drug for medical purposes. In this context, it is important to notice that sequence selectivity can occur through 3 distinct ways of direct readout of H-bond structure, indirect readout of structural flexibility and a combination of both [30,34]. Most of current docking programs (e.g. AutoDockVina) do not take into account the receptor flexibility. Therefore, our presented data are only valid for the first way of sequence selectivity. Additional experiments such as crystallographic, biochemical and spectroscopic experiments are suggested to elucidate the exact mechanisms of the sequence selectivity of FO.

In this study, vascular alteration in the CAM of chick embryos was seen following FO treatment. Morphometrical analysis of the CAM vasculature showed that FO negatively affected vessels percentage area and total vessels length. The histopathological evaluation was also confirmed the anti-angiogenic property of FO, because significant reduction of vasculature was seen in H&E and reticulin staining. This altered vascular plexus may provide a relation between FO administration and its toxicity, which was observed in some other studies. In this respect, various macroscopic and microscopic lesions have been reported following FO administration in chick embryo [26], human [6,10,35–37] and mice/rat [38].

In the present study, analysis of the CAM vasculature and calculation of the MCA were the two methods applied to quantify the anti-angiogenic effect of FO. To date, these methods have been widely used in vascular evaluations [26,39–41]. Moreover, the time of treatment was chosen based on the previously documented times in which vascular alterations have been noted and the embryo is more susceptible to teratogens [2,28,42,43].

FO administration caused a significant alteration in the normal expression of angiogenic-regulating gene (e.g. VEGF-A). The mechanisms and pathways by which FO alters angiogenesis is not clearly defined; however, based on our *in silico* study in which FO was shown to be bonded to the active site of VEGF-A protein and WTI binding sites by van der Waals and hydrogen bonds, the anti-angiogenic activity of FO can be attributed to: 1) alteration in VEGF-A expression and 2) interaction with VEGF-A protein and promoter.

In the present paper, interaction between FO, VEGF-A protein and promoter was proved by docking assay. Therefore, it is suggested that FO can alter the function of VEGF-A related pathway. However, further studies (e.g. protein level examination, biochemical examination, immunohistochemistry study and crystallographic investigation) are required to support our results. Our findings may provide important recommendations for future researches.

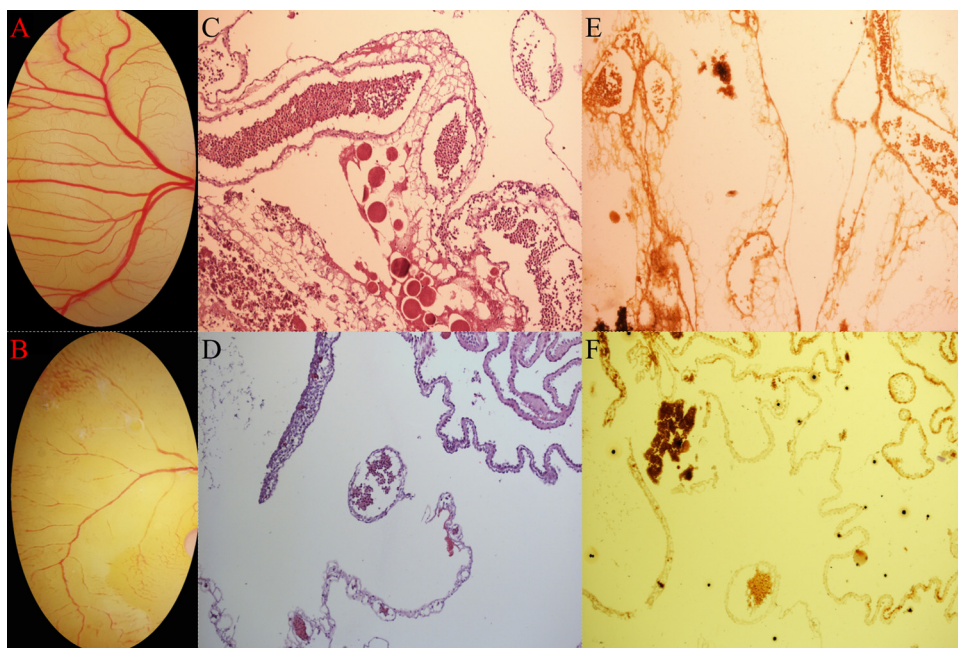


Fig. 9. Histopathological results of H&E and reticulin staining (A) Normal embryo CAM in control group (B) abnormal embryo CAM in fosfomycin treated group (C) H&E staining on control group showed well vascularization vessels filled by RBC and leukocytes, with prominent endothelial cells (D) H&E staining of treated group by fosfomycin showed significantly decreased vasculature (E and F) Reticulin staining confirmed H&E finding that fosfomycin treated group has significantly decreased vasculature compare control group.

The phrase "chick embryo model" was used in the current paper for two purposes: to clarify the vascular toxicity of the FO in the chick embryo and to put special emphasis on the benefits of using the chick embryo model in medical studies. In details, determination of the effects of drugs in biological systems requires a preclinical model. Because of the low cost, simplicity, reduced ethical and legal aspects and good reproducibility of the results, the chick embryo provides an appropriate model for in vivo evaluation of the activity, pharmacokinetics, biodistribution, biocompatibility and toxicity of the drugs [44–47]. These data have made chick embryo as an available model for genomic comparison in human and other species.

Using a chick embryo model, our study confirmed the anti-angiogenic effect of FO. Despite the negative concept of this effect, FO as an antiangiogenic agent may suppress tumor growth. In agreement with this assumption, some antineoplastic activities (e.g. cancer pro-coagulant inhibitor and anti-neoplastic activity in bone cancer) were predicted for FO when its structure was uploaded onto PASS online software. Certainly, this potential will shed new light on cancer therapy. However, it needs further pharmaceutical studies.

As far as the authors are aware, the current research is the first one to target the anti-angiogenic effect of FO in a chick embryo model. Our results indicate that FO not only interferes with angiogenic factors, but also adversely affects the normal regulation of the angiogenic gene and results in devastating consequences (e.g. vascular alteration). The presented data on anti-angiogenic effect of FO permit us to recommend the restriction on FO administration in poultry breeder farms or its cautious use. Consequently, safe alternatives should be considered. However, from another perspective, anti-angiogenic effect of FO with its sequence-selective property may give rise to very promising results in cancer treatments.

Declaration of Competing Interest

There is no competing interest.

Acknowledgments

The authors would like to thank the Clinical Science Research Center personnel as well as Dr. Balal Sadeghi for their helpful assistance and advice throughout this study. This research was financially supported by Shahid Bahonar University of Kerman, Kerman, Iran (project

no. 95-P/11/20).

References

- [1] J.E. Riviere, M.G. Papich, *Veterinary Pharmacology and Therapeutics*, John Wiley & Sons, 2018.
- [2] A. Khosravi, I. Sharifi, H. Tavakkoli, A.R. Keyhani, A. Afgar, Z. Salari, S.S. Mosallanejad, M. Bamorovat, F. Sharifi, S. Hassanzadeh, B. Sadeghi, S. Dabiri, A. Mortazaeizadeh, Z. Sheikhsheoae, E. Salarkia, Vascular apoptosis associated with meglumine antimoniate: in vivo investigation of a chick embryo model, *Biochem. Biophys. Res. Commun.* 505 (2018), <https://doi.org/10.1016/j.bbrc.2018.09.152>.
- [3] J. Mesquita, J.P. Castro-de-Sousa, S. Vaz-Pereira, A. Neves, L.A. Passarinha, C.T. Tomaz, Vascular endothelial growth factors and placenta growth factor in retinal vasculopathies: current research and future perspectives, *Cytokine Growth Fact. Rev.* 39 (2018) 102–115.
- [4] B. Rashidi, M. Malekzadeh, M. Goodarzi, A. Masoudifar, H. Mirzaei, Green tea and its anti-angiogenesis effects, *Biomed. Pharmacother.* 89 (2017) 949–956.
- [5] V.L.N. David, E. Swayne, J.R. Glisson, L.R. McDougald, L.K. Nolan, D.L. Suarez, *Diseases of Poultry*, Wiley-Blackwell, 2013.
- [6] T. Mayama, M. Yokota, I. Shimatani, H. Ohyagi, Analysis of oral fosfomycin calcium (Fosmicin) side-effects after marketing, *Int. J. Clin. Pharmacol. Ther. Toxicol.* 31 (1993) 77–82.
- [7] A. Eryilmaz, M. Durdu, M. Baba, N. Bal, F. Yiğit, A case with two unusual findings: cutaneous leishmaniasis presenting as panniculitis and pericarditis after antimony therapy, *Int. J. Dermatol.* 49 (2010) 295–297.
- [8] A. Matsumori, S. Yoneda, Y. Kobayashi, K. Takeda, M. Andoh, Y. Yamane, K. Nishimura, H. Kojima, H. Fukui, A case of acute severe hepatitis induced by fosfomycin, *Nihon Shokakibyō Gakkai Zasshi = Jpn. J. Gastro-Enterol.* 102 (2005) 1207–1211.
- [9] H. Tavakkoli, A. Derakhshanfar, S. Noori Gooshki, Toxicopathological lesions of fosfomycin in embryonic model, *Eur. J. Exp. Biol.* 4 (2014) 63–71.
- [10] D. Iarikov, R. Wassel, J. Farley, S. Nambiar, Adverse events associated with fosfomycin use: review of the literature and analyses of the FDA adverse event reporting system database, *Infect. Dis. Ther.* 4 (2015) 433–458.
- [11] M. El-sayed, Some Adverse Effects of Fosfomycin in Rats, (2016).
- [12] S. Dieguez, A. Soraci, A. Cristófar, M.O. Tapia, G. Martinez, F.B. Paggi, R. Harkes, fosfomycin residues and withdrawal time in eggs after oral administration to laying hens: 5.3, *J. Vet. Pharmacol. Ther.* 38 (2015) 113.
- [13] C. Betz, A. Lenard, H.-G. Belting, M. Affolter, Cell behaviors and dynamics during angiogenesis, *Development* 143 (2016) 2249–2260.
- [14] F.C. Brunicardi, Angiogenesis review commentary, *World J. Surg.* 41 (2017) 1635.
- [15] J.Q. Chen, L.H. Huang, Advances of researchs on molecular mechanisms of mesenchymal stem cells and their exosomes in angiogenesis—review, *Zhongguo Shi Yan Xue Ye Xue Za Zhi* 26 (2018) 1858–1862.
- [16] I.Y.Y. Koh, V.A. Eylich, M.A. Marti-Renom, D. Przybylski, M.S. Madhusudhan, N. Eswar, O. Grana, F. Pazos, A. Valencia, A. Sali, EVA: evaluation of protein structure prediction servers, *Nucleic Acids Res.* 31 (2003) 3311–3315.
- [17] J. Hanson, J. Gorman, J. Reese, G. Fraizer, Regulation of vascular endothelial growth factor, VEGF, gene promoter by the tumor suppressor, WT1, *Front. Biosci. J. Virt. Libr.* 12 (2007) 2279.
- [18] X. Messegueur, R. Escudero, D. Farré, O. Nuñez, J. Martínez, M.M. Albá, PROMO: detection of known transcription regulatory elements using species-tailored

- searches, *Bioinformatics* 18 (2002) 333–334.
- [19] D. Farré, R. Roset, M. Huerta, J.E. Adsuara, L. Roselló, M.M. Albà, X. Messeguer, Identification of patterns in biological sequences at the ALGGEN server: PROMO and MALGEN, *Nucleic Acids Res.* 31 (2003) 3651–3653.
- [20] M. van Dijk, A.M.J.J. Bonvin, 3D-DART: a DNA structure modelling server, *Nucleic Acids Res.* 37 (2009) W235–W239.
- [21] O. Trott, A.J. Olson, AutoDock Vina: improving the speed and accuracy of docking with a new scoring function, efficient optimization, and multithreading, *J. Comput. Chem.* 31 (2010) 455–461.
- [22] M. Coll, J. Aymami, G.A. Van der Marel, J.H. Van Boom, A. Rich, A.H.J. Wang, Molecular structure of the netropsin-d (CGCGATATCGCG) complex: DNA conformation in an alternating AT segment, *Biochemistry* 28 (1989) 310–320.
- [23] A. Canals, M. Purciolas, J. Aymami, M. Coll, The anticancer agent ellipticine unwinds DNA by intercalative binding in an orientation parallel to base pairs, *Acta Crystallogr. Sect. D: Biol. Crystallogr.* 61 (2005) 1009–1012.
- [24] C. Su, P. Zhang, J. Liu, Y. Cao, Erianin inhibits indoleamine 2, 3-dioxygenase-induced tumor angiogenesis, *Biomed. Pharmacother.* 88 (2017) 521–528.
- [25] A.M. Oosterbaan, E.A.P. Steegers, N.T.C. Ursem, The effects of homocysteine and folic acid on angiogenesis and VEGF expression during chicken vascular development, *Microvasc. Res.* 83 (2012) 98–104.
- [26] A. Khosravi, I. Sharifi, H. Tavakkoli, A. Derakhshanfar, A.R. Keyhani, Z. Salari, S.S. Mosallanejad, M. Bamorovat, Embryonic toxico-pathological effects of meglumine antimoniate using a chick embryo model, *PLoS One* 13 (2018), <https://doi.org/10.1371/journal.pone.0196424>.
- [27] S. Bagés, J. Estany, M. Tor, R.N. Pena, Investigating reference genes for quantitative real-time PCR analysis across four chicken tissues, *Gene* 561 (2015) 82–87.
- [28] A.K. Gheorghescu, B. Tywoniuk, J. Duess, N.-V. Buchete, J. Thompson, Exposure of chick embryos to cadmium changes the extra-embryonic vascular branching pattern and alters expression of VEGF-A and VEGF-R2, *Toxicol. Appl. Pharmacol.* 289 (2015) 79–88.
- [29] E.K. Barbour, Z. El-Hajj, H. Shaib, H. Itani, M. Saadeh, W. Haidar, L. Jaber, R. Demloj, S. Harakeh, Impact of synergism of calcium phosphomycin/tylosin tartrate supplements on the performance of broilers in the Lebanon, *Vet. Ital.* 46 (2010) 45–49.
- [30] C.T. Winston, D.L. Boger, Sequence-selective DNA recognition: natural products and nature's lessons, *Chem. Biol.* 11 (2004) 1607–1617.
- [31] M.J. Hannon, Supramolecular DNA recognition, *Chem. Soc. Rev.* 36 (2007) 280–295.
- [32] C. Bailly, J.B. Chaires, Sequence-specific DNA minor groove binders. Design and synthesis of netropsin and distamycin analogues, *Bioconjug. Chem.* 9 (1998) 513–538.
- [33] J. Alvar, S. Yactayo, C. Bern, Leishmaniasis and poverty, *Trends Parasitol.* 22 (2006) 552–557.
- [34] O. Norberto de Souza, R.L. Ornstein, Inherent DNA curvature and flexibility correlate with TATA box functionality, *Biopolym. Org. Res. Biomol.* 46 (1998) 403–415.
- [35] M.J. Rosales, F. Vega, Anaphylactic shock due to fosfomycin, *Allergy* 53 (1998) 905–907.
- [36] S. Durupt, R.N. Jossierand, M. Sibille, I. Durieu, Acute, recurrent fosfomycin-induced liver toxicity in an adult patient with cystic fibrosis, *Scand. J. Infect. Dis.* 33 (2001) 391–392.
- [37] M.E. Falagas, E.K. Vouloumanou, G. Samonis, K.Z. Vardakas, Fosfomycin, *Clin. Microbiol. Rev.* 29 (2016) 321–347.
- [38] T. Koeda, M. Odaki, H. Sasaki, M. Yokota, H. Watanabe, H. Kawaoto, T. Ito, N. Ishiwatari, Toxicological studies on fosfomycin-Na salt. I. Acute toxicity in mice and rats (author's transl), *Jpn. J. Antibiot.* 32 (1979) 61–66.
- [39] M. Seifaddinipour, R. Farghadani, F. Namvar, J. Mohamad, H. Abdul Kadir, Cytotoxic effects and anti-angiogenesis potential of pistachio (*Pistacia vera* L.) hulls against MCF-7 human breast cancer cells, *Molecules* 23 (2018) 110.
- [40] F.K. de S.L. Borba, G.L.Q. Felix, E.V.L. Costa, L. Silva, P.F. Dias, R. de Albuquerque Nogueira, Fractal analysis of extra-embryonic vessels of chick embryos under the effect of glucosamine and chondroitin sulfates, *Microvasc. Res.* 105 (2016) 114–118.
- [41] H. Tavakkoli, J. Tajik, M. Zeinali, Evaluating the effects of Enrofloxacin on angiogenesis using the chick embryo chorioallantoic membrane model, *Iran. J. Vet. Surg.* 11 (2016) 17–22.
- [42] M.N. Nazem, R. Amanollahi, H. Tavakoli, F. Mansouri, Effect of in ovo injected methionine on feather follicle formation and its growth in the chicken embryo, *Anat. Sci. J.* 12 (2015) 83–88.
- [43] D. Geng, A.A. Musse, V. Wigh, C. Carlsson, M. Engwall, M. Orešič, N. Scherbak, T. Hyötyläinen, Effect of perfluorooctanesulfonic acid (PFOS) on the liver lipid metabolism of the developing chicken embryo, *Ecotoxicol. Environ. Saf.* 170 (2019) 691–698.
- [44] S.A. Mousa, M. Yalcin, P.J. Davis, Models for assessing anti-angiogenesis agents: appraisal of current techniques, *Anti-Angiogenesis. Strateg. Cancer Ther.* Elsevier, 2017, pp. 21–38.
- [45] R.B. Knight, S. Dvorcakova, L. Luptakova, K. Vdoviakova, V. Petrilla, E. Petrovova, Evaluation of vasoactivity after haemotoxic snake venom administration, *Toxicol. Appl. Pharmacol.* 158 (2019) 69–76.
- [46] S. Maacha, S. Saule, Evaluation of tumor cell invasiveness in vivo: the chick chorioallantoic membrane assay, *Cell Migr.* Springer, 2018, pp. 71–77.
- [47] D. Ribatti, R. Tamma, The chick embryo chorioallantoic membrane as an in vivo experimental model to study human neuroblastoma, *J. Cell. Physiol.* 234 (2019) 152–157.